symmetry

MDPI

Article

The Role of Urban Expansion and Groundwater Conditions in the Spatial Distribution of Building Damage During the 6 February 2023 Kahramanmaraş Earthquakes

Erdem Gündoğdu [1], Aydın Büyüksaraç [1], Ercan Işık [2], Fatih Avcil [2,*] and Marijana Hadzima-Nyarko [3,*]

[1] Department of Mining and Mineral Extraction, Çan Vocational School, Çanakkale Onsekiz Mart University, 17400 Çanakkale, Türkiye
[2] Department of Civil Engineering, Faculty of Engineering and Architecture, Bitlis Eren University, 13100 Bitlis, Türkiye
[3] Faculty of Civil Engineering and Architecture, Josip Juraj Strossmayer University of Osijek, 31000 Osijek, Croatia
* Correspondence: favcil@beu.edu.tr (F.A.); mhadzima@gfos.hr (M.H.-N.)

Abstract

The city center of Kahramanmaraş suffered considerable damage as a result of the Mw 7.7 Pazarcık and Mw 7.6 Elbistan earthquakes, which took place on 6 February 2023. The present study examines the impact of urban development, groundwater conditions, and paleo-drainage systems on the pattern of earthquake damage in the Dulkadiroğlu and Onikişubat districts, which make up the urban center of Kahramanmaraş. Geological, hydrogeological, geomorphological, urban development, and building damage data were combined and analyzed using a GIS environment. Kernel Density Estimation (KDE) and spatial overlay analyses were carried out in order to show the spatial concentration of the damage. The results show that severely damaged or collapsed buildings were not distributed at random; rather, they were found in regions featuring largely young geological units, shallow groundwater levels, and former stream channels. In several areas where rapid urban expansion has occurred over the past thirty years, there is a clear spatial relationship between high damage densities and paleo-drainage systems. These findings reveal a spatial relationship between severe building damage and areas characterized by alluvial deposits, reconstructed paleo-drainage corridors, and potentially shallow groundwater conditions. Although the available data do not allow the damage to be directly attributed to site amplification or other geotechnical mechanisms, the observed spatial patterns identify areas where local ground conditions warrant further geotechnical and seismological investigation.

Keywords: Kahramanmaraş earthquakes; damage distribution; paleo-drainage; urban expansion; land use change; spatial distribution

Check for updates

Academic Editor: Vasilis K. Oikonomou

Received: 8 August 2026
Revised: 27 August 2026
Accepted: 7 September 2026
Published: 9 September 2026

Copyright: © 2026 by the authors. Licensee MDPI, Basel, Switzerland. This article is an open access article distributed under the terms and conditions of the Creative Commons Attribution (CC BY) license.

1. Introduction

Ground motion characteristics and soil–structure interaction are frequently addressed through soil profiles and symmetric/asymmetric behavior patterns under dynamic loading. The propagation of seismic waves, ground amplification, and the spatial distribution of building damage caused by earthquakes cannot be explained solely by theoretical homogeneity assumptions such as proximity to faults or superstructure quality; rather, they are driven by complex geotechnical asymmetries created by anthropogenic factors such

as paleodrain lines, shallow groundwater levels, and uncontrolled urban expansion [1–7]. This study aims to examine the spatial clustering of building damage observed during the 6 February 2023 Kahramanmaraş earthquakes in an integrated manner with the effects of urban area expansion, hydrogeological conditions, and buried streambeds on dynamic soil behavior. Revealing how natural geological/hydrogeological irregularities and urban growth patterns disrupt symmetrical approaches in soil mechanics and shape spatial asymmetry in damage distribution is a critical requirement and of paramount importance for seismic risk mitigation strategies, microzonation studies, and resilient urban planning.

The Mw 7.7 and Mw 7.6 Kahramanmaraş earthquakes that occurred on 6 February 2023 have been recorded as one of the most devastating disasters in the recent history of Türkiye. Affecting a large part of Southern and South-eastern Anatolia as well as northern Syria, these earthquakes caused extensive loss of life, severe structural damage, and significant socio-economic consequences [8–11]. Although numerous studies have investigated the source mechanisms and tectonic characteristics of the earthquakes [12–20], the pronounced variations in damage distribution observed within urban centers indicate that the destruction cannot be explained solely by earthquake magnitude, distance from the fault, or building quality. The fact that structures located in proximity experienced markedly different levels of damage suggests that local geological, hydrogeological, and geomorphological conditions exert significant control on ground behaviour during earthquakes [21]. Kahramanmaraş city center represents one of the most striking examples of this phenomenon [22]. In recent decades, the city has undergone rapid urban expansion, particularly toward alluvial plains, former stream channels, and areas characterized by shallow groundwater levels. This uncontrolled growth process has led to substantial modifications of both surface and subsurface environments through anthropogenic interventions such as the alteration of natural drainage systems, the creation of artificial fill areas, intensive urbanization, and changes in groundwater regimes [23]. These modifications are thought to have increased seismic vulnerability in urban areas by amplifying ground motion and reducing soil strength during earthquake events.

Previous studies have demonstrated that local ground conditions, groundwater levels, and sedimentological characteristics directly influence processes such as seismic wave amplification, liquefaction potential, and differential settlement [24–28]. In particular, water-saturated unconsolidated alluvial deposits may experience significant reductions in shear strength under repeated dynamic loading, leading to severe ground deformation. Furthermore, former river channels and buried paleo-drainage systems may become zones of concentrated damage during earthquakes due to their high moisture content and weak mechanical properties. In rapidly urbanizing areas such as Kahramanmaraş, the interaction between urban development processes and hydrogeological conditions is considered one of the key factors controlling the spatial distribution of earthquake damage [29]. In addition, urbanization processes substantially modify the natural hydrological balance. The expansion of impermeable surfaces, disruption of natural infiltration processes, alteration of surface drainage networks, and increasing structural loads can directly affect the engineering properties of subsurface materials. Consequently, the damage distribution observed following major earthquakes often reflects not only tectonic factors but also the complex interactions among ground conditions, groundwater behavior, former drainage systems, and unplanned urbanization.

In the case of the 6 February 2023 Kahramanmaraş earthquakes, the combined effects of urban development and groundwater conditions on earthquake damage have not been fully explored. Most research so far has looked at structural engineering, active tectonics, or regional seismotectonic features. However, there has been less focus on how hydrogeological conditions and past urbanization patterns affect the spread of damage. Learning

more about these connections is important for future microzonation studies, disaster risk reduction, and sustainable urban planning.

The primary objective of this study is to investigate the influence of urban development processes and groundwater conditions on the spatial distribution of damage observed during the 6 February 2023 Kahramanmaraş earthquakes. By integrating geological, hydrogeological, geomorphological, and urban development data, the study aims to investigate how these factors are spatially associated with local earthquake damage patterns. The findings are expected to contribute not only to the interpretation of post-earthquake damage distribution but also to the development of sustainable urbanization strategies and earthquake risk reduction efforts in Türkiye and other regions with similar tectonic settings.

The novelty of this study lies in the integration of reconstructed paleo-drainage corridors and historical urban expansion with geological, hydrogeological, geomorphological, and building-damage datasets within a unified GIS framework. Rather than considering earthquake damage solely from a structural or tectonic perspective, this approach examines how the historical development of the urban area intersects with former geomorphological features and present-day ground conditions. This integrated perspective provides a spatial basis for identifying areas where the relationship between urban development, paleo-drainage, local ground conditions, and earthquake damage warrants further investigation.

2. Geological and Geomorphological Characteristics of the Study Area

The city center of Kahramanmaraş is situated within a complex geomorphological environment that has developed under the influence of active tectonic processes associated with the East Anatolian Fault Zone (EAFZ) (Figure 1). The city is generally located within a transitional zone between the mountainous terrains rising to the north and west and the extensive alluvial plains extending toward the south and east. This setting results in pronounced topographic and geological variations over relatively short distances within the urban area.

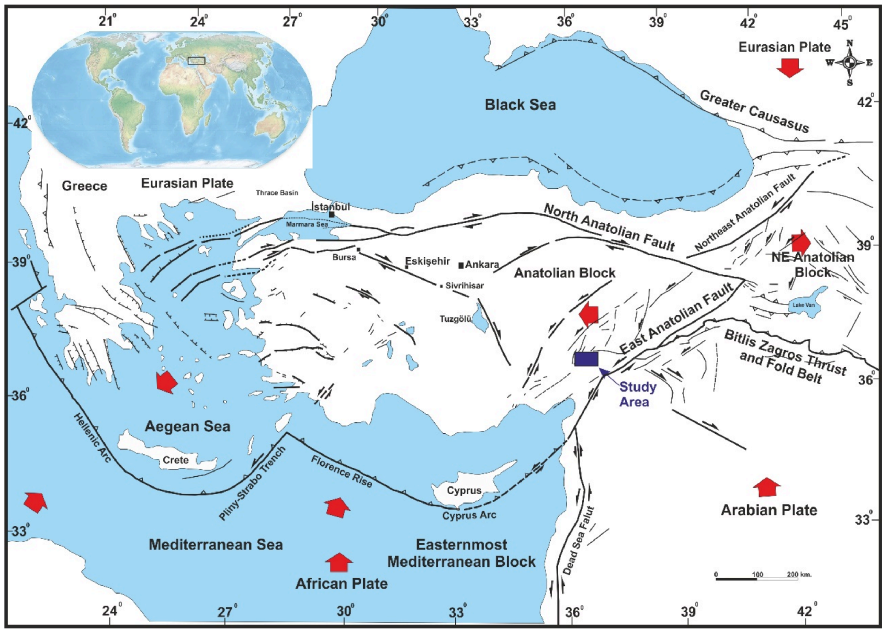


Figure 1. Location of the study area on the active tectonic elements in and around Anatolia (modified from [30–32]).

A significant part of the city center has developed on young Quaternary alluvial deposits transported and accumulated by fluvial systems. These alluvial units consist of

unconsolidated sediments such as clay, silt, sand, and gravel, and exhibit poor geotechnical properties in areas characterized by high groundwater levels. In particular, along former stream channels, floodplains, and paleo-drainage systems, increased soil saturation and loose sediment structure may increase susceptibility to ground-motion amplification, differential settlement, and liquefaction; however, these mechanisms are not directly evaluated in the present study.

The formation of the Kahramanmaraş Plain is largely controlled by tectonic processes. Active faulting in the region has led to the development of subsidence areas, which were subsequently infilled by thick alluvial deposits over time (Figure 2). Consequently, the depth to bedrock locally increases significantly beneath the city center, resulting in the accumulation of thick sedimentary sequences. These thick alluvial deposits can amplify low-frequency seismic waves, thereby increasing earthquake-induced damage [24,33]. Between 6 February 2023 and 26 May 2026, a total of 37 earthquakes with Mw $\geq$ 5.0 occurred in and around Kahramanmaraş, including two events with Mw $\geq$ 7.0 and one event with Mw $\geq$ 6.0 (Table 1).

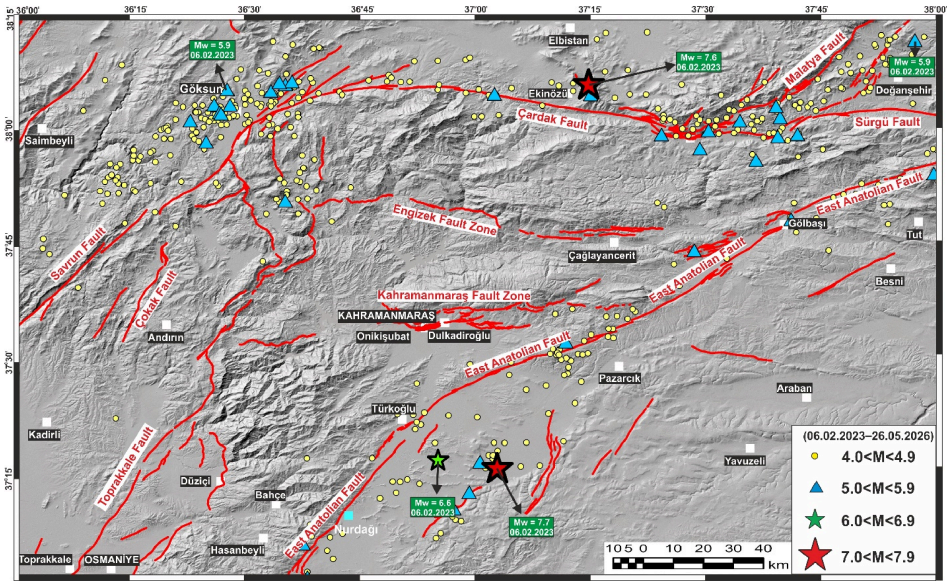


Figure 2. The main tectonic elements and active fault segments along with the East Anatolian Fault Zone (modified from [34,35]). The red lines delineate the major active faults. The dark red circles denote city center.

Table 1. Earthquakes with Mw $\geq$ 5.0 ranked by magnitude (AFAD Earthquake Catalog; accessed 26 May 2026). (M: Magnitude, A1: Adana, K: Kahramanmaraş, A2: Adıyaman, M: Malatya, G: Gaziantep, O: Osmaniye, Lon: Longitude, Lat: Latitude) (Adapted from [36]).

Date	Lon	Lat	Depth	Rms	Type	M	Location
24 May 2026 04:26	36.09	37.75	9.32	0.54	M_W	4.9	Saimbeyli (A1)
7 September 2024 09:31	37.04	37.27	7.00	0.34	M_W	5.0	Pazarcık (K)
3 May 2023 20:16	36.56	38.06	7.00	0.59	M_W	5.0	Göksun (K)
23 March 2023 12:19	36.44	38.03	12.90	0.73	M_W	5.3	Göksun (K)
3 March 2023 05:53	36.59	37.83	7.06	0.34	M_W	5.0	Onikişubat (K)
27 February 2023 05:51	37.58	37.92	8.51	0.54	M_W	5.0	Gölbaşı (A2)
18 February 2023 22:31	36.59	38.07	6.20	0.29	M_W	5.1	Göksun (K)
8 February 2023 17:20	37.38	37.97	16.69	0.20	M_L	5.0	Nurhak (K)
8 February 2023 14:11	37.63	38.00	13.18	0.35	M_L	5.3	Doğanşehir (M)

Table 1. *Cont.*

Date	Lon	Lat	Depth	Rms	Type	M	Location
8 February 2023 10:48	36.45	38.02	9.06	0.30	M_W	5.1	Göksun (K)
8 February 2023 00:21	37.46	37.94	15.84	0.39	M_W	5.0	Nurhak (K)
7 February 2023 21:09	36.61	38.08	10.22	0.83	M_W	5.0	Göksun (K)
7 February 2023 18:48	36.43	37.95	11.48	0.56	M_W	5.2	Göksun (K)
7 February 2023 06:13	37.65	37.79	8.44	0.37	M_W	5.4	Gölbaşı (A2)
7 February 2023 06:08	37.62	37.97	6.87	0.30	M_W	5.0	Doğanşehir (M)
7 February 2023 00:15	37.03	38.05	17.40	0.49	M_W	5.0	Ekinözü (K)
6 February 2023 23:37	37.04	37.28	5.96	0.43	M_W	5.5	Pazarcık (K)
6 February 2023 21:05	36.39	38.00	7.03	0.14	M_W	5.0	Göksun (K)
6 February 2023 21:03	36.48	38.03	12.79	0.37	M_W	5.2	Göksun (K)
6 February 2023 19:43	36.46	38.01	10.06	0.43	M_W	5.1	Göksun (K)
6 February 2023 18:14	37.66	37.97	7.04	0.46	M_W	5.0	Doğanşehir (M)
6 February 2023 16:44	37.54	38.00	8.76	0.45	M_W	5.1	Nurhak (K)
6 February 2023 16:39	37.62	38.03	7.20	0.52	M_W	5.3	Doğanşehir (M)
6 February 2023 16:17	36.58	38.08	10.85	0.55	M_W	5.2	Göksun (K)
6 February 2023 15:13	37.48	37.98	7.00	0.30	M_W	5.1	Nurhak (K)
6 February 2023 15:02	36.47	38.06	17.04	0.93	M_W	5.9	Göksun (K)
6 February 2023 13:35	37.91	38.17	11.28	0.78	M_W	5.9	Doğanşehir (M)
6 February 2023 13:32	37.23	38.05	10.93	0.88	M_L	5.5	Ekinözü (K)
6 February 2023 13:24	37.230	38.07	7.00	0.58	M_W	7.6	Elbistan (K)
6 February 2023 09:54	37.45	37.73	7.00	0.49	M_W	5.0	Çağlayancerit (K)
6 February 2023 05:23	36.94	37.19	11.81	0.32	M_W	5.3	Nurdağı (G)
6 February 2023 05:03	37.95	37.89	10.23	0.58	M_W	5.6	Doğanşehir (M)
6 February 2023 05:01	37.00	37.29	16.44	0.85	M_W	5.3	Pazarcık (K)
6 February 2023 04:58	36.64	37.05	10.21	0.44	M_W	5.3	İslâhiye (G)
6 February 2023 04:51	37.18	37.54	6.63	0.92	M_W	5.3	Dulkadiroğlu (K)
6 February 2023 04:36	36.63	37.12	11.19	0.29	M_L	5.7	Hasanbeyli (O)
6 February 2023 04:28	36.91	37.29	6.20	0.21	M_W	6.6	Nurdağı (G)
6 February 2023 04:26	36.98	37.22	6.98	0.42	M_L	5.6	Nurdağı (G)
6 February 2023 04:17	37.03	37.27	8.60	1.92	M_W	7.7	Pazarcık (K)

Examination of the topography of the city center reveals abrupt slope transitions from steep hillside areas to the adjacent plain surface. These morphological transition zones control both surface and groundwater flow patterns and influence sediment accumulation processes. Furthermore, the loss of natural drainage functions in former stream channels, which were active in the past but are now largely covered by urban development, may have contributed to the concentration of subsurface moisture in certain parts of the city.

Another notable geomorphological aspect is the substantial modification of the natural topography by urbanization. Landfills channelized or buried stream courses, alterations to surface drainage systems, and intensive urban development have disrupted natural geomorphological processes, potentially affecting ground behavior during earthquakes. In particular, unplanned construction on alluvial fill areas is considered one of the key factors controlling the spatial distribution of earthquake damage. The city center of Kahramanmaraş is situated between the steep slopes of Ahır Mountain to the north and the alluvial plain to the south. Streams descending from the northern high-relief terrain generate large volumes of surface runoff within a short period. Therefore, the city is exposed to a chronic flood hazard not only because of intense rainfall events but also due to its topographic setting. As urban expansion progressed northward, highly permeable areas became increasingly covered by impervious surfaces. Hillslopes that previously absorbed rainfall have largely lost their infiltration capacity. Consequently, stormwater now reaches the city center much more rapidly. This process can be interpreted less as a conventional 'natural disaster' and more as a 'human-induced disaster amplification mechanism [23].

The natural drainage pattern within the study area is predominantly oriented from north to south and southeast. Numerous short and steep tributary streams descend from the northern highlands and enter the urban area. Within the city, many of these channels have been narrowed, diverted into culverts, or completely infilled. The principal alluvial-fan drainage system originates from the slopes of Ahır Mountain, where numerous small streams converge upon entering the city center. In the north-eastern sector, the Peynirdere Basin and its associated tributaries merge with other drainage branches in the central part of the city. Most of these channels have been converted into culverted or roadside drainage systems, while some have disappeared entirely from the surface landscape. The eastern sector contains the largest drainage catchments and represents the area most susceptible to flooding, characterized by extensive alluvial fans and low-gradient confluence zones. Consequently, streams in this sector possess a particularly high potential for damage generation. Many former stream channels have been buried beneath roads and urban infrastructure and are now covered by dense development (Figure 3). In Kahramanmaraş, stream channels have not disappeared; rather, they have been concealed beneath the modern urban fabric.

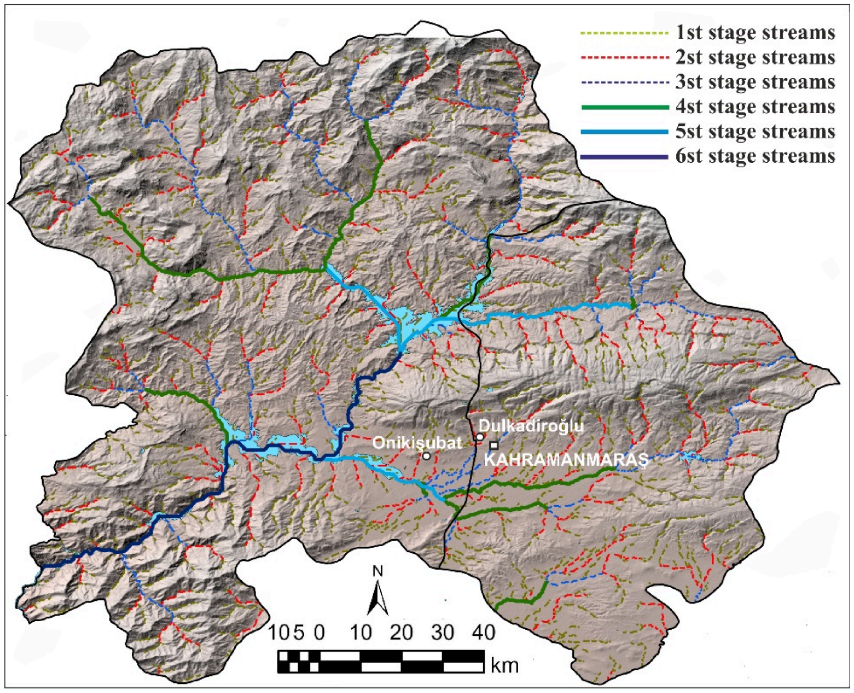


Figure 3. Geomorphological map of the Kahramanmaraş city center, including the Dulkadiroğlu and Onikişubat districts and their surrounding areas. Digital Elevation Model (SRTM 1 Arc-Second Global) data were downloaded from [37]. Subsequently, hydrological analyses were performed in ArcGIS Pro 3.6.0 using the sequential processing steps of Flow Direction, Flow Accumulation, Stream Order, and Stream to Feature.

The spatial coincidence between DEM-derived paleo-drainage corridors, alluvial fan deposits, mapped active fault zones, and severe building damage suggests that the 2023 earthquake damage pattern in central Kahramanmaraş was strongly modulated by inherited geomorphological and structural controls rather than by seismic source proximity alone. The reconstructed paleo-drainage network reveals that a significant portion of the urbanized areas in Kahramanmaraş is located along buried fluvial corridors, which coincide with low-lying topographic depressions and alluvial deposits, suggesting a strong coupling between geomorphological inheritance, subsurface heterogeneity, and seismic damage distribution.

3. Methodological Framework

This study investigates the relationship between the damage distribution observed following the 6 February 2023 Kahramanmaraş earthquakes and urban development, groundwater conditions, and paleo-drainage systems. For this purpose, geological, geomorphological, hydrogeological, urban development, and building damage datasets were integrated within a Geographic Information System (GIS) environment. A Digital Elevation Model (DEM) with a spatial resolution of 30 m was obtained from the USGS Earth Explorer database. The spatial evolution of urban development was analysed using historical and recent satellite imagery covering the period from 1985 to 2025. Building damage inventories compiled after the 2023 earthquakes were obtained from the Ministry of Environment, Urbanization and Climate Change. Damage data were classified into four categories: moderately damaged, heavily damaged, buildings requiring urgent demolition, and collapsed buildings.

Hydrological analyses were conducted using ArcGIS Pro software. In the first stage, sink-filling and preprocessing procedures were applied to the DEM data. Subsequently, the Flow Direction and Flow Accumulation algorithms were employed to determine surface runoff pathways. The paleo-drainage network was reconstructed using the Stream Order and Stream to Feature tools, enabling the identification of buried or anthropogenically modified drainage corridors underlying the present-day urban area. Particular attention was focused on former stream channels that have been infilled, covered, or opened to urban development in recent decades. The urban growth process between 1985 and 2025 was digitized and analysed using satellite imagery. Urban boundaries corresponding to the selected years were delineated and compared to identify the principal directions of urban expansion. Particular attention was given to the extent to which urban growth has encroached upon alluvial plains, former drainage corridors, and areas characterized by high groundwater levels.

Urban growth rates and expansion patterns were examined separately for the Dulkadiroğlu and Onikişubat districts. Geomorphological units, including alluvial plains, alluvial fans, valley fills, floodplains, and colluvial deposits, were mapped using DEM-based topographic analyses and existing geological data. Given the 30 m spatial resolution of the DEM, the resulting hydrological analysis was considered appropriate for identifying regional drainage patterns and broader paleo-drainage corridors, but not for resolving narrow or deeply buried stream channels beneath dense urban infrastructure. Therefore, the mapped paleo-drainage features were interpreted as indicative corridors rather than precise channel boundaries. The identification of areas potentially characterized by shallow groundwater conditions was based on available hydrogeological and geomorphological information rather than direct, site-specific groundwater-level measurements collected after the earthquake. Therefore, the present study does not directly quantify groundwater depth or temporal groundwater fluctuations at individual building locations. Areas potentially characterized by shallow groundwater conditions were identified using hydrogeological maps, drainage density, topographic depressions, and geomorphological indicators. Areas with a high potential for groundwater concentration were compared with paleo-drainage corridors and damage clusters to examine their spatial associations and to identify areas where potential local site effects may warrant further geotechnical and seismological investigation.

Building damage data were imported into the GIS environment and overlaid with geomorphological, hydrogeological, and urban development layers. Kernel Density Estimation (KDE) was applied to identify the spatial concentration of damage. Buffer zones were

generated around paleo-drainage corridors to investigate the spatial relationship between former stream channels and damaged buildings.

$$\hat{f}(x) = \frac{1}{nh^2}\sum_{i=1}^{n} K\left(\frac{x - x_i}{h}, \frac{y - y_i}{h}\right) \quad (1)$$

Because the building damage locations are represented as two-dimensional spatial coordinates, KDE was implemented as a bivariate density estimation. Accordingly, the normalization term is, where represents the bandwidth, and denotes the bivariate kernel function. The spatial distance between each building location and the evaluation location was calculated using the distance metric used in the GIS analysis. The KDE therefore estimates the spatial density of damaged buildings as a function of the two-dimensional distribution of building locations.

Bandwidth (h) is the parameter that most strongly influences KDE results. Smaller bandwidth values produce highly detailed but potentially noisy patterns, whereas larger bandwidth values generate smoother and more generalized results. For each damage category, the number and proportion of buildings located within the influence zones of paleo-drainage features were calculated. Comparative analyses were also conducted between the Dulkadiroğlu and Onikişubat districts. Spatial overlay and frequency analyses were applied to quantitatively assess the influence of environmental factors on damage distribution. The proportions of damaged buildings located within alluvial units, paleo-drainage corridors, and shallow groundwater zones were calculated. The effects of environmental factors were evaluated by comparing heavily damaged and collapsed buildings with moderately damaged buildings. Through the integrated interpretation of geological, geomorphological, hydrogeological, and urban development datasets, the environmental control mechanisms contributing to increased earthquake damage were identified. The methodological framework of the study consists of eight stages (Figure 4).

The present analysis primarily focuses on the spatial distribution of building damage in relation to geological, hydrogeological, geomorphological, and urban-development characteristics. Building-level structural variables, including construction age, structural system, number of storeys, and detailed construction quality, were not systematically incorporated into the spatial statistical analysis. Therefore, the observed relationships should be interpreted as spatial associations rather than independent causal effects of geological or hydrogeological conditions. The present dataset does not allow the quantitative separation of structural vulnerability associated with the older building stock in Dulkadiroğlu from potential site-related effects associated with paleo-drainage corridors. Building age, structural system, number of storeys, and other building-level characteristics may act as confounding factors. Therefore, the observed spatial association between damage and paleo-drainage corridors is interpreted cautiously and is not considered independent evidence of site amplification.

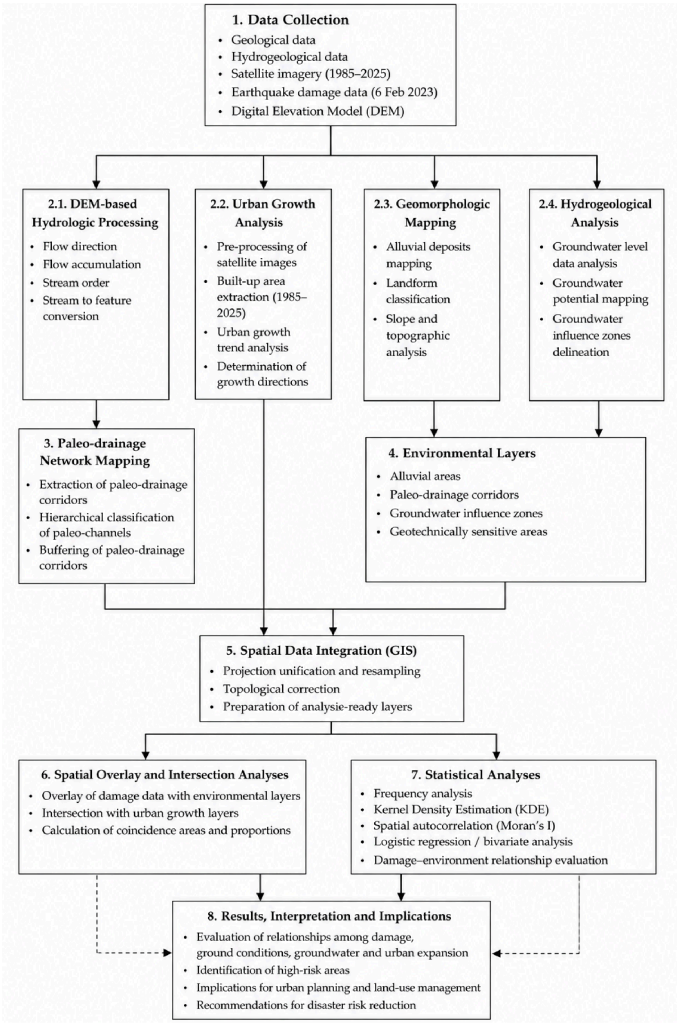


Figure 4. Methodological workflow illustrating the integration of urban expansion, groundwater conditions, paleo-drainage mapping, and earthquake damage data for investigating the spatial distribution of building damage in the Kahramanmaraş city center following the 6 February 2023 earthquakes.

4. Urban Development and Land Use Change in Kahramanmaraş

The Dulkadiroğlu and Onikişubat districts, which together constitute the urban center of Kahramanmaraş, have experienced significant urban growth over the last five decades as a result of rapid population increase, rural-to-urban migration, and the concentration of economic activities. Dulkadiroğlu, which forms the historical core of the city, developed as the area where traditional urban fabric, commercial districts, and older neighbourhoods are concentrated. Public institutions, historic bazaar areas, and the older residential building stock are particularly abundant in this district. However, topographic constraints and the high density of aging buildings have contributed to an unplanned and compact urbanization pattern. In contrast, Onikişubat has become the focal area of westward urban expansion, particularly since the 1990s. Wide boulevards, mass housing developments, university campuses, shopping centers, and new social and recreational spaces have largely been concentrated within this district. The city's modern growth corridor has generally expanded toward the northwest and west, into areas characterized by gentler slopes, contributing to a more planned and horizontally developed urban structure in Onikişubat. The urban development processes of both districts have been reassessed following the 2023 Türkiye–Syria earthquakes.

In particular, the influence of geomorphological and geotechnical factors, including alluvial deposits, former stream channels, groundwater conditions, and site amplification effects, on building damage has prompted a re-evaluation of urban planning policies.

While the concentration of older and densely built structures in Dulkadiroğlu was found to have amplified earthquake impacts, the newer development areas in Onikişubat were generally more systematically planned; nevertheless, severe damage was still observed in several areas underlain by alluvial deposits. Figure 5 illustrates the evolution of urban building development in Kahramanmaraş between 1985 and 2025. The results indicate that urban expansion has intensified particularly on the western side of the city since 2004, whereas in older residential areas, low-rise structures have progressively been replaced by multi-storey mass housing developments.

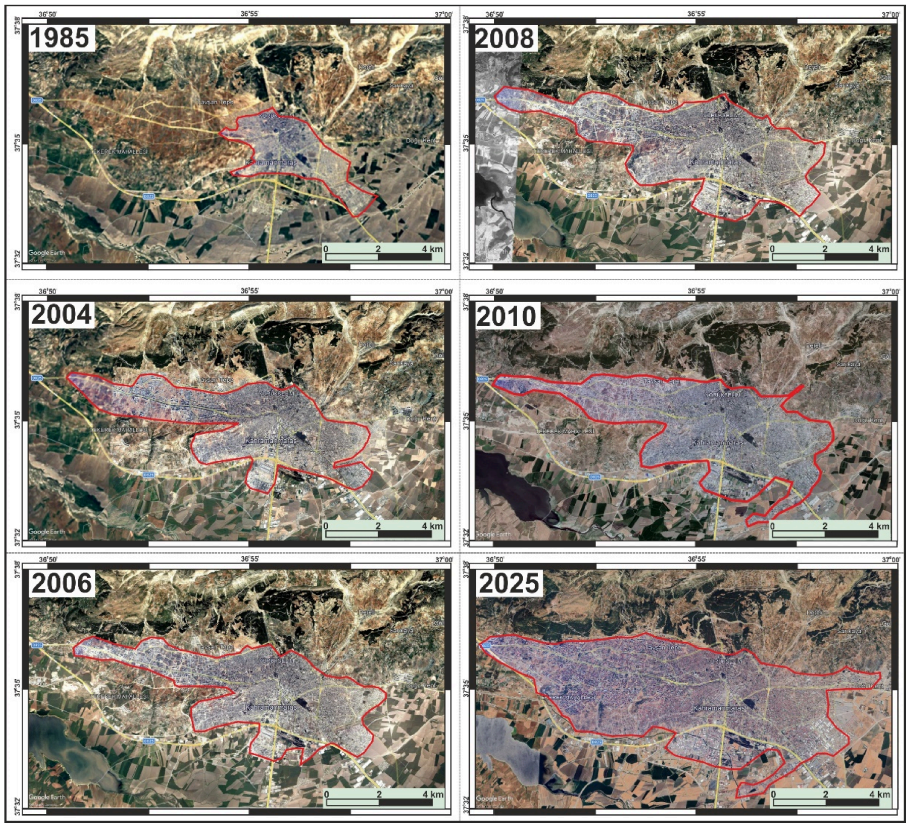


Figure 5. A Google Earth image showing the evolution of Kahramanmaraş's urban building stock between 1985 and 2025. Basemap imagery © Google Earth and the imagery provider(s) indicated in the original image.

At present, the urban development of Kahramanmaraş continues to be influenced by population growth, expanding transportation infrastructure, university and industrial investments, and disaster risk management policies. In the aftermath of the earthquakes, site suitability assessments, microzonation studies, and sustainable urban planning strategies have emerged as critical factors guiding the future development of both districts.

5. Spatial Distribution of Building Damage During the 6 February 2023 Earthquakes

The Mw 7.7 Pazarcık earthquake that occurred on 6 February 2023 and the Mw 7.6 Elbistan earthquake that followed approximately nine hours later have been recorded as one of the most devastating disasters in the recent history of Türkiye. The earthquakes caused extensive loss of life and property across a broad region, particularly in Kahramanmaraş,

Hatay, Adıyaman, Malatya, and Gaziantep, with tens of thousands of buildings collapsing or sustaining severe damage. The events developed along with a multi-segment rupture system associated with the East Anatolian Fault Zone and generated surface ruptures extending for several hundred kilometers. The first earthquake, centered near Pazarcık, and the second earthquake, centered near Elbistan, produced strong ground motions with high acceleration levels over a very large area. At several strong-motion stations, recorded ground-motion intensities and spectral accelerations reached exceptionally high levels, locally exceeding the levels anticipated by the design spectra, thereby imposing severe seismic demands on structures. Near-fault effects, rupture directivity, and the complex rupture propagation contributed to exceptionally strong and spatially variable ground motions, thereby increasing seismic demands on structures in the affected region [38–40].

The distribution of earthquake damage in and around the Kahramanmaraş city center is not homogeneous. While some neighbourhoods experienced extensive destruction, nearby areas suffered relatively limited damage. This pattern can be explained not only by earthquake magnitude but also by the combined influence of multiple factors, including ground conditions, groundwater levels, building stock characteristics, building age, and construction quality. A substantial proportion of the damaged structures consisted of reinforced-concrete buildings constructed before 2000. Common structural deficiencies observed in these buildings included inadequate transverse reinforcement detailing, low concrete strength, short-column effects, soft-story irregularities, and the failure to satisfy the strong-column/weak-beam design principle. Consequently, damage levels varied even among areas subjected to similar levels of ground shaking. Table 2 presents the proportions of four different damage categories in the Dulkadiroğlu and Onikişubat districts. The proportions of collapsed buildings, buildings requiring urgent demolition, and heavily damaged buildings are significantly higher in the Dulkadiroğlu district. In contrast, the proportion of moderately damaged buildings is higher in the Onikişubat district. Although these district-level ratios cannot replace the grid-based damage ratio recommended by the reviewer, they provide a normalized comparison that accounts for the substantial difference in total building stock between the two districts.

Table 2. Distribution of building damage categories between the Dulkadiroğlu and Onikişubat districts. Percentages are calculated by row and represent the proportion of buildings in each district relative to the total number of buildings within each damage category (Adapted from [41,42]).

Damage Type	Dulkadiroğlu	Damage Ratio (%)	Onikişubat	Damage Ratio (%)
Total building stock [42]	98,655		164,507	
Moderately damaged buildings	1281	1.29	1364	0.83
Heavily damaged buildings	7061	7.15	5333	3.24
Buildings requiring urgent demolition	1121	1.13	502	0.30
Collapsed buildings	1514	1.53	753	0.45
Overall Total	10,977	11.12	7952	4.83

The observed damage pattern clearly reveals a higher concentration of severe damage in the older urban districts. Although substantial damage can be expected from a sequence of large earthquakes generating exceptionally strong ground motions [43–45], the unusually high proportion of collapsed and heavily damaged buildings may also reflect deficiencies in construction practices, the vulnerability of the existing building stock, and insufficient consideration of local geotechnical conditions [46–56]. Figure 6 illustrates the spatial distribution of the different damage categories observed within the Kahramanmaraş city center. To further examine whether the observed concentration of earthquake damage

is associated with the underlying geological setting, the spatial distribution of damaged buildings shown in Figure 6 was additionally evaluated with respect to the mapped geological units. Because a complete inventory of the total number of buildings located within each individual geological unit was not available, a conventional damage ratio (damaged buildings/total buildings within each geological unit) could not be calculated reliably. Instead, the proportion of the observed damaged buildings associated with the mapped geological units, including Q, M-cc, and M-nl units, was calculated relative to the total number of damaged buildings. This analysis provides a relative description of how the observed damaged buildings are distributed among the mapped geological units.

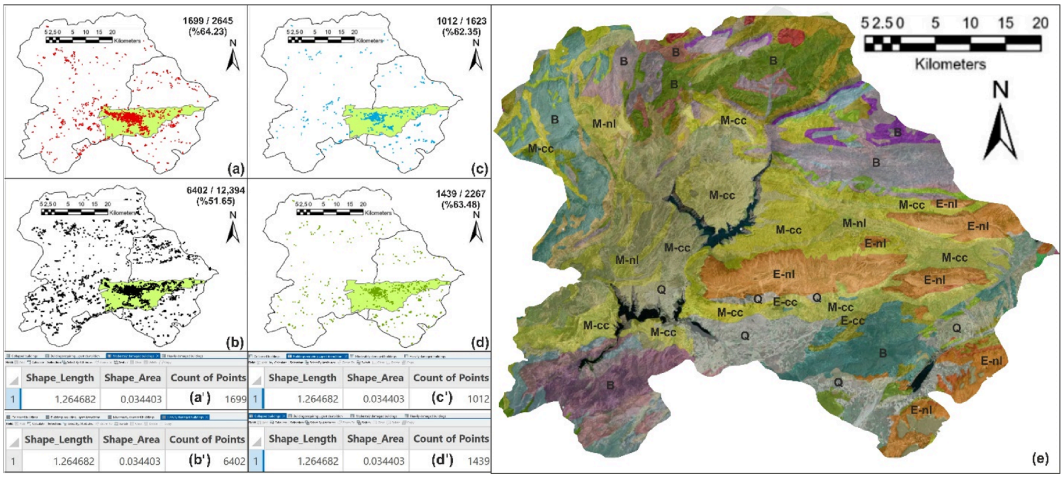


Figure 6. Damage distribution in the Kahramanmaraş city center and the Dulkadiroğlu (D) and Onikişubat (O) districts. (**a**,**a′**) Moderately damaged buildings (D: 1281; O: 1364; Total: 2645), (**b**,**b′**) Heavily damaged buildings (D: 7061; O: 5333; Total: 12,394), (**c**,**c′**) Buildings requiring urgent demolition (D: 1121; O: 502; Total: 1623), and (**d**,**d′**) Collapsed buildings (D: 1514; O: 753; Total: 2267). The shaded areas in (**a**–**d**) indicate the building conditions within the young geological units from the Miocene and later periods. (**e**) Geological map of the study area (simplified from [57] (Q: Quaternary units, M-cc: Miocene clastic and carbonate rocks, M-nl: Miocene neritic limestone, E-cc: Eocene clastic and carbonate rocks, E-nl: Eocene neritic limestone, B: Pre-Eocene basement units).

The results indicate that a substantial proportion of the heavily damaged, urgently demolishable, and collapsed buildings is spatially concentrated within the Quaternary/alluvial settings, whereas comparatively lower proportions of severe damage are observed in areas underlain by older geological units. This pattern is particularly relevant in Onikişubat, where severe damage is also observed in relatively recently developed urban areas located on alluvial deposits. The persistence of severe damage in these areas suggests that building age and urban density alone may not fully explain the observed spatial pattern. Taken together, these results support a spatial association between local geological conditions and the observed distribution of earthquake damage.

However, this spatial association should not be interpreted as evidence of a direct causal effect, because the total building stock within individual geological units was not available for normalization. Therefore, the results represent the relative distribution of observed damage among geological units rather than a building-level probability of damage. Similarly, the analysis does not independently quantify site amplification or other geotechnical mechanisms. The observed pattern is consequently interpreted as spatial evidence supporting a possible association between local geological conditions and damage distribution, while the independent contributions of building age, structural system, number of storeys, and construction quality remain unresolved.

The statistical distribution of damage is shown in Figure 7a–c. The spatial overlap zone where high concentrations of all four damage categories (moderately damaged, heavily damaged, buildings requiring urgent demolition, and collapsed buildings) coexist in the Dulkadiroğlu and Onikişubat districts was identified and illustrated in Figure 8. The area, bounded by 36.90–37.00° E and 37.55–37.60° N, was subsequently examined in detail, and the distribution of all buildings within this overlap zone is presented in Figure 9.

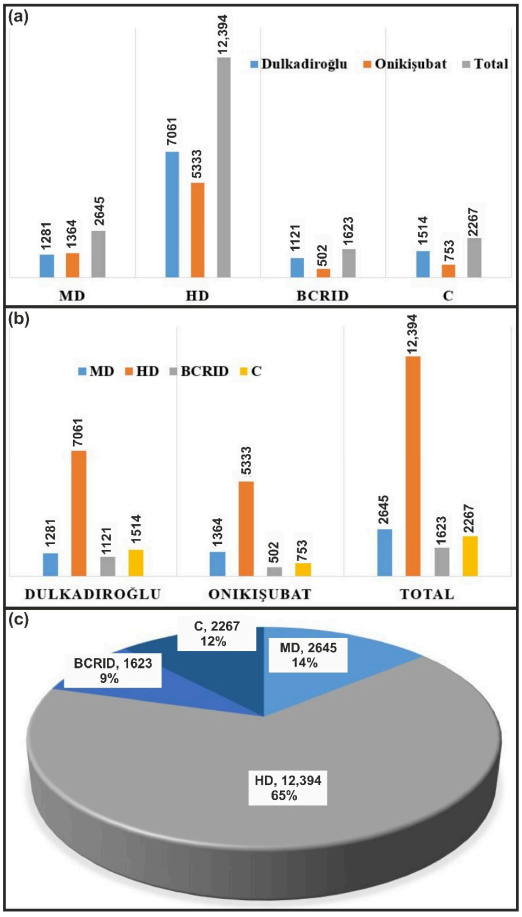


Figure 7. Damage distribution statistics (**a**) District-based distribution of building types, (**b**) distribution of building types in the districts, (**c**) proportional distribution of building types in the districts (MD: Moderately damaged buildings, HD: Heavily damaged buildings, BCRID: Buildings requiring urgent demolition, C: Collapsed buildings).

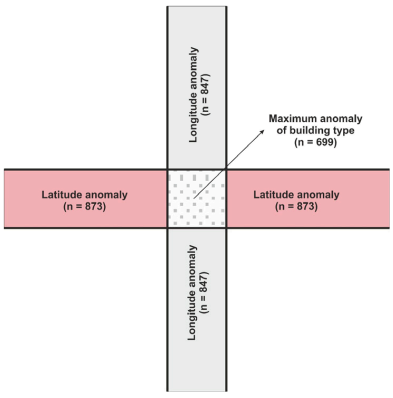


Figure 8. Schematic illustration of the procedure used to identify the overlap area between zones of high damage concentration along the latitude and longitude directions, shown for collapsed buildings in the Dulkadiroğlu district as an example.

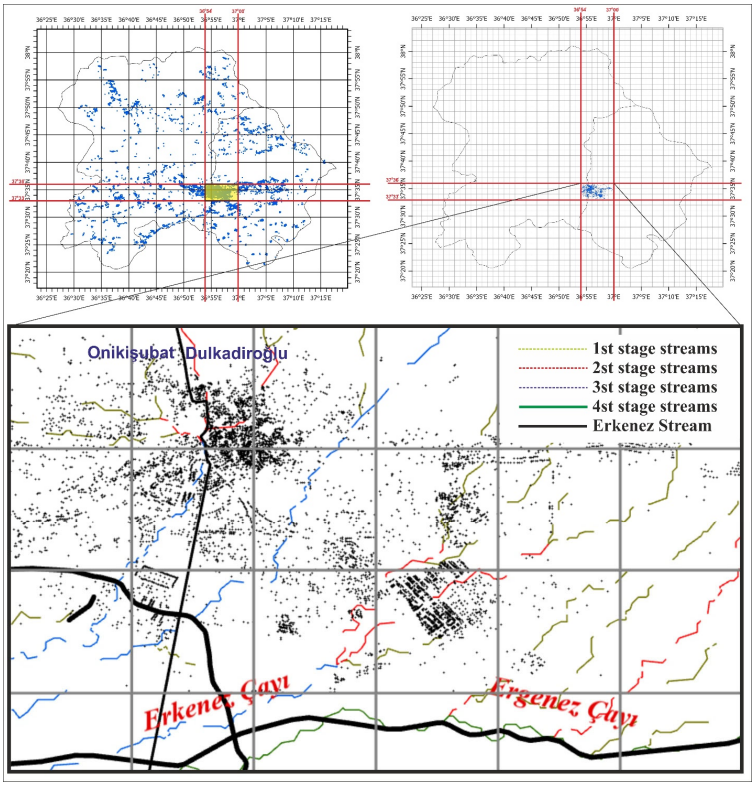


Figure 9. Spatial distribution of all damaged building categories (18,929 buildings) in the Dulkadiroğlu and Onikişubat districts and the subset located within the identified overlap zone (7309 buildings).

As shown in Figure 9, buildings located within the identified overlap zone are predominantly concentrated in areas north of the present-day Erkenez (Ergenez) Stream, which are largely underlain by Quaternary deposits. In addition to the current course of the Erkenez (Ergenez) Stream, drainage networks numbered 1–4, described in detail in Figure 3, are densely distributed within this area. These drainage features represent former streams, abandoned stream channels, and paleodrainage corridors. Approximately 48.92% of the four damage categories identified within the Dulkadiroğlu district are located inside this overlap zone, whereas the corresponding proportion for the Onikişubat district is 24.38%. The proportions of the different building damage categories within the entire districts and within the overlap zone are presented in Table 3.

Table 3. Proportions of building damage categories within the overlap area (36.90–37.00° E, 37.55–37.60° N) in the Dulkadiroğlu and Onikişubat districts.

Damage Level	Dulkadiroğlu			Onikişubat		
	Number of Buildings	Number of Buildings Within the Overlap Area	Rate (%)	Number of Buildings	Number of Buildings Within the Overlap Area	Rate (%)
Moderately damaged buildings	1281	700	54.64	1364	331	24.27
Heavily damaged buildings	7061	3535	50.06	5333	972	18.23
Buildings requiring urgent demolition	1121	436	38.89	502	203	40.44
Collapsed buildings	1514	699	46.17	753	433	57.50
Overall Total	10,977	5370	48.92	7952	1939	24.38

Figure 10 illustrates the district- and neighbourhood-scale distribution of damage categories within the area bounded by 36.90–37.00° E and 37.55–37.60° N, where damaged buildings are most densely concentrated in the Onikişubat and Dulkadiroğlu districts.

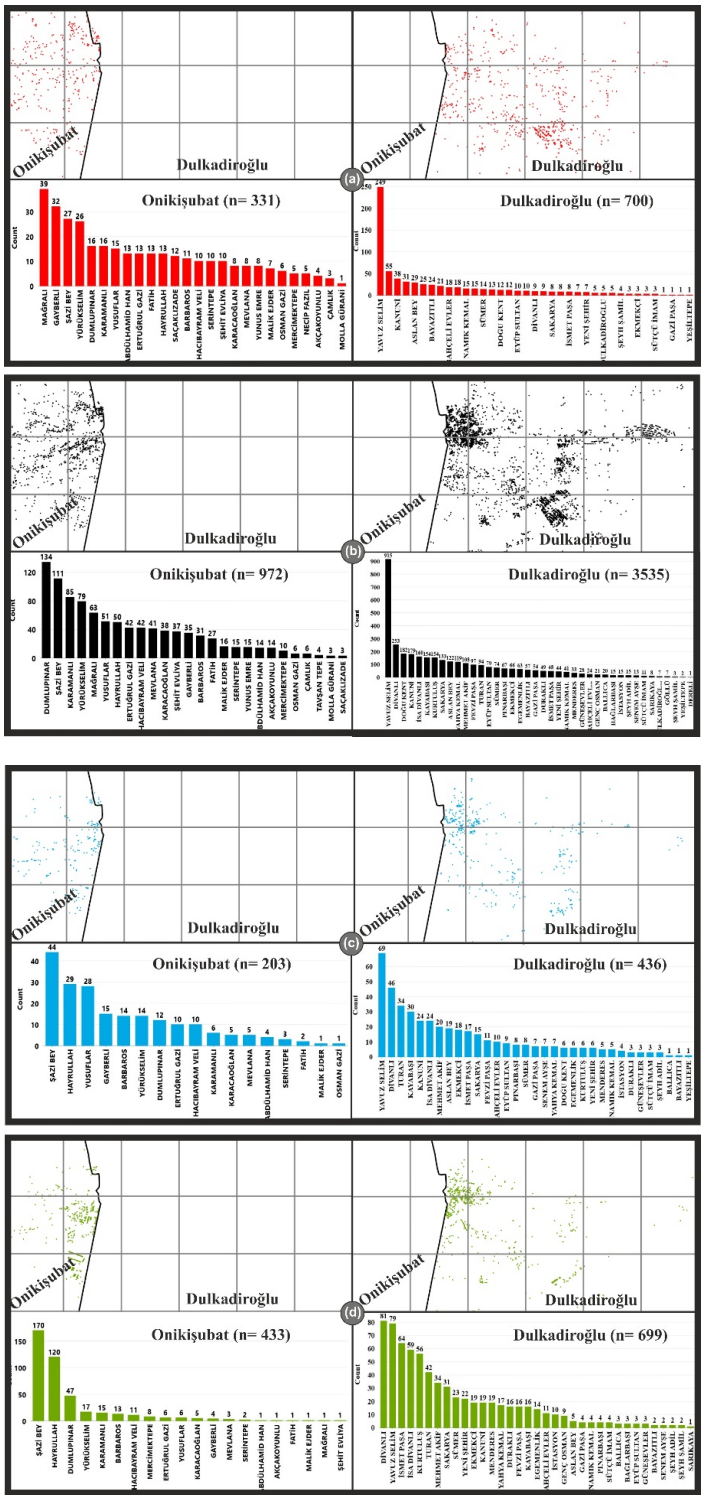


Figure 10. District- and neighbourhood-scale distribution of damage categories within the area bounded by 36.90–37.00° E and 37.55–37.60° N, where damaged buildings are concentrated in the Onikişubat and Dulkadiroğlu districts: (**a**) Moderately damaged buildings, (**b**) Heavily damaged buildings, (**c**) Buildings requiring urgent demolition, and (**d**) Collapsed buildings.

6. Conclusions

This study comprehensively evaluated the effects of urban development processes, paleo-drainage systems, and groundwater conditions on the spatial distribution of earthquake damage observed in the city center during the 6 February 2023 Kahramanmaraş earthquakes. The spatial analysis indicates that earthquake damage is associated with a combination of ground-motion conditions, building characteristics, and geological, hydrogeological, and geomorphological settings. However, the relative contribution of these factors cannot be quantitatively separated using the available dataset. Although strong ground motions were recorded during the 6 February 2023 earthquakes, site-specific PGA, PGV, spectral acceleration, or empirical site-amplification parameters were not incorporated into the present spatial analysis. Consequently, the observed damage concentrations cannot be directly attributed to differences in local ground motion. Similarly, the present study does not include SPT/CPT data, shear-wave velocity measurements, laboratory testing, or a quantitative liquefaction-triggering assessment. Therefore, the paleo-drainage and shallow-groundwater zones identified here should be considered areas of potential geotechnical interest rather than confirmed liquefaction-affected areas.

A substantial part of the Kahramanmaraş city center has developed on young Quaternary alluvial deposits. DEM-based hydrological analyses revealed that paleo-drainage corridors identified within the study area are currently covered by dense urbanization, and a considerable proportion of these corridors coincide with zones that experienced severe damage during the earthquakes. Lose and potentially water-saturated soil conditions associated with former stream channels and alluvial fan systems may have influenced local ground response during the earthquakes. The concentration of severe building damage within areas underlain by Quaternary alluvial deposits and paleo-drainage corridors suggests that local ground conditions may be associated with the observed damage pattern. However, in the absence of site-specific bedrock-depth measurements, subsurface soil profiles, shear-wave velocity data, and quantitative site-response analyses, the potential role of these deposits in low-frequency seismic-wave amplification cannot be directly demonstrated. Urban growth analyses indicate that, particularly during the last four decades, the city has expanded onto natural drainage systems and alluvial plains. During this process, many stream channels were narrowed, culverted, or completely occupied by urban development. Modification of the natural drainage network has not only increased flood susceptibility but has also altered subsurface water circulation and soil moisture conditions, thereby influencing ground behaviour during seismic events.

Damage statistics reveal that the proportions of heavily damaged, urgently demolishable, and completely collapsed buildings are significantly higher in the Dulkadiroğlu District than in the Onikişubat District. The main reasons for this difference include the concentration of older building stock, unplanned urbanization, high building density, and unfavorable ground conditions. In contrast, relatively lower levels of severe damage were observed in Onikişubat due to the presence of newer residential developments. Nevertheless, significant damage was also recorded in some newly developed areas situated on alluvial deposits, emphasizing the possible role of local ground conditions in earthquake performance. The occurrence of substantial damage in some relatively recent development areas located on alluvial deposits suggests that building age alone may not fully explain the observed spatial pattern. Nevertheless, because building-level structural characteristics were not systematically controlled for, the relative contributions of building vulnerability and local ground conditions cannot be independently quantified in the present study.

The results indicate that the spatial distribution of earthquake damage in the Kahramanmaraş city center is associated with a combination of complex interactions among active tectonics, alluvial sediment thickness, paleo-drainage systems, groundwater condi-

tions, and building stock characteristics. In particular, buried stream channels and areas characterized by shallow groundwater levels appear to represent priority risk zones in terms of seismic hazard. Groundwater flowing from adjacent slopes tends to follow structural weakness zones, which are predominantly associated with alluvial deposits. These conditions may indicate potential local site effects that require further investigation. The potential role of shallow groundwater should be interpreted with caution. The present study does not include systematic well-based groundwater-level measurements, piezometric observations, or site-specific hydrogeological monitoring at the damaged building locations. Therefore, the identified association between potential shallow groundwater conditions and damage concentration does not constitute direct evidence that groundwater levels amplified earthquake damage. Instead, these areas are considered zones where shallow groundwater may warrant further investigation using field-based groundwater measurements, geotechnical testing, and site-response analyses. Several areas that experienced concentrated damage during the 2023 earthquakes correspond spatially with artificial fill zones and former river channels.

The findings show that future urban renewal, microzonation, and disaster risk reduction studies should consider not only building characteristics but also paleo-drainage networks, groundwater conditions, and geomorphological processes. A detailed review of settlements located on former stream channels using advanced geotechnical and geophysical methods is key to reducing the impacts of future disasters. The Kahramanmaraş case demonstrates that natural environmental conditions and uncontrolled urban expansion can jointly increase seismic risk and provides notable scientific evidence for long-term urban planning.

In conclusion, the Kahramanmaraş city center is defined by a complex geomorphological setting formed by active tectonics, alluvial deposits, former drainage systems, shallow groundwater conditions, and accelerated urbanization. These factors provide an important structure for understanding the geographical variations in earthquake damage observed during the 6 February 2023 earthquakes.

The damage distribution in Kahramanmaraş is therefore not solely a consequence of earthquake magnitude but rather the combined effect of geological, geomorphological, and engineering factors. The observed spatial coincidence between severe building damage and alluvial deposits, paleo-drainage corridors, and areas potentially characterized by shallow groundwater suggests that local ground conditions may be associated with the spatial distribution of damage. However, the present analysis does not allow these relationships to be interpreted as direct causal effects or to independently quantify site amplification, liquefaction triggering, or other geotechnical mechanisms. Spatial association should not be interpreted as causal attribution, particularly in the absence of site-specific ground-motion, geotechnical, and building-level structural data. Future studies integrating site-specific ground-motion records, geophysical measurements, SPT/CPT data, groundwater observations, liquefaction assessments, and building-level structural characteristics are required to distinguish the relative contributions of local ground conditions and structural vulnerability. The results underline the crucial importance of microzonation studies, in-depth site investigations, and seismic performance assessments of existing building stocks for future disaster risk reduction strategies.

Author Contributions: Conceptualization, E.G., A.B. and E.I.; methodology, E.G., E.I., F.A. and A.B.; software, E.G. and F.A.; validation, M.H.-N. and E.I.; formal analysis, M.H.-N. and E.I.; investigation, E.G. and A.B.; writing—original draft preparation, E.G., A.B. and E.I.; writing—review and editing, F.A. and M.H.-N.; visualization, E.G. and F.A.; supervision, A.B. and M.H.-N. All authors have read and agreed to the published version of the manuscript.

Funding: This research received no external funding.

Data Availability Statement: The original contributions presented in this study are included in the article. Further inquiries can be directed to the corresponding authors.

Acknowledgments: ChatGPT (GPT-5.6 Luna) was used only for English translation and language editing of the manuscript. The authors reviewed and edited the AI-assisted text and take full responsibility for the final content of the manuscript.

Conflicts of Interest: The authors declare no conflicts of interest.

References

1. Metwaly, M.; Alshami, A. Paleoenvironmental Changes and Human Adaptation: A Multidisciplinary Investigation of Site Abandonment at Qusayrat Aad Archaeological Site, Central Saudi Arabia. *ISPRS Int. J. Geo-Inf.* **2026**, *15*, 334. [CrossRef]
2. Wang, X.; Zou, H.; Chen, H.; Cao, Y. Application of an Interpretable Machine Learning Model to Archaeological Site Prediction: A Case Study of the Three Gorges Region in Chongqing. *ISPRS Int. J. Geo-Inf.* **2026**, *15*, 329. [CrossRef]
3. Yang, J.; Luo, L.; Shao, J.; Wang, Y.; Chen, Q.; Fan, J.; Fu, X.; Tu, R.; Luo, Z.; Zhang, Z.; et al. Predictive Modeling of Han Dynasty Beacon Towers Accounting for Spatial Heterogeneity: A Geographically Weighted and GeoShapley-Interpretable Framework. *npj Herit. Sci.* **2026**. [CrossRef]
4. El-Haddad, B.A.; Youssef, A.M.; Mahran, T.M.; El-Sharter, A.; Pourghasemi, H.R. Mapping of the Pre-Eonile-Eonile Sediments Using Remote Sensing Technique and Sedimentological Investigation in the Western Desert of Egypt. *J. Afr. Earth Sci.* **2026**, *2026*, 106005. [CrossRef]
5. Nurtas, M.; Orynbassarova, E.; Mohammed, M.A.; Nurmakhambet, S.; Altaibek, A.; Serikbayeva, E.; Iskakov, B. Integrated Application of Artificial Intelligence and Remote Sensing Techniques for Improved Subsurface Resource Exploration. *Eng. Sci.* **2025**, *39*, 1948. [CrossRef]
6. Villate-Daza, D.A.; Barboza-Pinzon, E.G.; Jigena-Antelo, B.; Muñoz-Perez, J.J.; Anfuso, G.; Portz, L.C.; Afanador-Franco, F.; Manzolli, R.P. Coastal Dynamics and Geomorphology of the Pozos Colorados sector, Santa Marta: An Analysis of Sea Level Rise and Paleo-Shoreline. *Front. Mar. Sci.* **2025**, *12*, 1700038. [CrossRef]
7. Luppichini, M.; Capolongo, D.; Scardino, G.; Scicchitano, G.; Bini, M. Artificial Intelligence in Geomorphology: A Bibliometric Analysis of Trends, Techniques, and Global Research Patterns. *Geosciences* **2025**, *15*, 331. [CrossRef]
8. Dedeoglu, I.O. Evaluating Earthquake-Induced Damage in Hatay Following the 2023 Kahramanmaraş Earthquake Sequence: Tectonic, Geotechnical, and Structural Engineering Insights. *Appl. Sci.* **2025**, *15*, 9704. [CrossRef]
9. Nemutlu, O.F. Loss Analyses Associated with the Secondary Effect in Earthquake: A Case Study of Kahramanmaras Earthquake Sequences. *Earthq. Struct.* **2025**, *28*, 137–147. [CrossRef]
10. Bayrak, E.; Çelebi, O.; Kılıç, M.; Özer, Ç.; Aydın, A.C. The Strong Ground Motion and Structural Response Analysis of 06 February 2023 Pazarcık and Elbistan Earthquakes (Mw 7.7 and 7.6): A Case Study for Malatya–Türkiye, Eastern Anatolia. *Bull. Earthq. Eng.* **2025**, *23*, 359–389. [CrossRef]
11. Öztürk Kardoğan, P.S. Assessment of Earthquake-Induced Settlements and Liquefaction Triggered by the 6 February 2023 Kahramanmaraş Earthquakes in Gölbaşı (Adıyaman) and İskenderun (Hatay). *Geomat. Nat. Hazards Risk* **2026**, *17*, 2650129. [CrossRef]
12. Peker, F.Ü.; Yuzbasi, J.; Işık, E.; Avcil, F.; Büyüksaraç, A. Seismic performance assessment and strengthening of a residential RC building damaged in the 2023 Türkiye Earthquakes: A case study. *Sci. Rep.* **2026**, *16*, 23737. [CrossRef] [PubMed]
13. Goldberg, D.E.; Taymaz, T.; Reitman, N.G.; Hatem, A.E.; Yolsal-Çevikbilen, S.; Barnhart, W.D.; Irmak, T.S.; Wald, D.J.; Öcalan, T.; Yeck, W.L.; et al. Rapid Characterization of the February 2023 Kahramanmaraş, Türkiye, Earthquake Sequence. *Seism. Rec.* **2023**, *3*, 156–167. [CrossRef]
14. Kobayashi, T.; Munekane, H.; Kuwahara, M.; Furui, H. Insights on the 2023 Kahramanmaraş Earthquake, Turkey, from InSAR: Fault Locations, Rupture Styles and Induced Deformation. *Geophys. J. Int.* **2024**, *236*, 1068–1088. [CrossRef]
15. Karabacak, V.; Özkaymak, Ç.; Sözbilir, H.; Tatar, O.; Aktuğ, B.; Özdağ, Ö.C.; Çakir, R.; Aksoy, E.; Koçbulut, F.; Softa, M.; et al. The 2023 Pazarcık (Kahramanmaraş, Türkiye) earthquake (Mw 7.7): Implications for Surface Rupture Dynamics along the East Anatolian fault zone. *J. Geol. Soc.* **2023**, *180*, jgs2023-020. [CrossRef]
16. Köküm, M. Kinematic and Dynamic Fault Slip Analyses: Implications from the Surface Rupture of the 2023 Elbistan (Kahramanmaraş) (Mw7. 6) Earthquake, Türkiye. *J. Struct. Geol.* **2024**, *187*, 105235. [CrossRef]
17. Utkucu, M.; Durmuş, H.; Uzunca, F.; Nalbant, S.; Arman, H. Time-dependent Coulomb stress changes background of the February 6, 2023 Pazarcık (Mw= 7.8) and Elbistan (Mw= 7.8) earthquakes in the southeast Türkiye. In *Proceedings of the Seventh International Conference on Engineering Geophysics, Al Ain, UAE, 16–19 October 2023*; Society of Exploration Geophysicists: Tulsa, OK, USA, 2023; pp. 152–155.

18. Nalbant, S.S.; Uzunca, F.; Main, I.G.; Utkucu, M.; Durmuş, H. Stress-Mediated Multi-Fault Rupture Dynamics of the 2023 Kahramanmaraş Earthquake Sequence, Türkiye. *Sci. Rep.* **2026**, *16*, 10705. [CrossRef] [PubMed]
19. Akinci, A.; Dindar, A.A.; Bal, I.E.; Ertuncay, D.; Smyrou, E.; Cheloni, D. Characteristics of Strong Ground Motions and Structural Damage Patterns from the February 6th, 2023 Kahramanmaraş Earthquakes, Türkiye. *Nat. Hazards* **2025**, *121*, 1209–1239. [CrossRef]
20. Kürçer, A.; Yalçın, H.D.; Elmacı, H.; Özalp, S.; Budakoğlu, E.; Güneş, Y.; Yıldırım, N.; Kayadibi, Ö. The 2020 Sivrice Earthquake (Mw6. 8) and Its Seismotectonic Linkage to the 2023 Kahramanmaraş Earthquakes (MW7. 8 and 7.6). *Nat. Hazards* **2026**, *122*, 220. [CrossRef]
21. Pamuk, E.; Fırat, S.; Büyüksaraç, A.; Çetin, K.Ö.; Bektaş, Ö.; Işık, N.S.; Sarıtepe, H.E. Three dimensional Shear Wave Velocity (Vs) Structure and Dynamic Soil Properties of Adıyaman-Gölbaşı Basin Using HVSR and SPAC Methods. *Soil Dyn. Earthq. Eng.* **2026**, *200*, 109744. [CrossRef]
22. Aras, F.; Doğan, T.P.; Öztürk, M.; Tün, M.; Işık, E.; Arslan, M.H. Assessment of The Damage Caused by the 6 February 2023 Earthquakes on Old and New Dated Reinforced Concrete Buildings in Elbistan, Turkey. *Adv. Struct. Eng.* **2026**, *29*, 1336–1363. [CrossRef]
23. Sarıgül, O.; Turoğlu, H. Flashflood and Flood Geographical Analysis and Foresight in Kahramanmaraş City. *Coğrafya Derg.* **2020**, *40*, 275–293. [CrossRef]
24. Över, S.; Büyüksaraç, A.; Bektaş, Ö.; Filazi, A. Assessment of Potential Seismic Hazard and Site Effect in Antakya (Hatay Province), SE Turkey. *Environ. Earth Sci.* **2011**, *62*, 313–326. [CrossRef]
25. Büyüksaraç, A.; Över, S.; Geneş, M.C.; Bikçe, M.; Kaçın, S.; Bektaş, Ö. Estimating shear Wave Velocity Using Acceleration Data in Antakya (Turkey). *Earth Sci. Res. J.* **2014**, *18*, 99–105. [CrossRef]
26. Coruk, Ö.; Ulutaş, E.; Gül, T. Engineering Geology and Ground Response Characterization along the Iskenderun Plain Triggered by the 2023 Pazarcık, Türkiye Earthquake. *J. Afr. Earth Sci.* **2026**, *2026*, 106083. [CrossRef]
27. Satriyo, N.A.; Mulyono, A.; Wibawa, S.; Yuliyanti, A.; Sari, A.M.; Putra, M.H.Z.; Arfiyansyah, K. The Review of the Geological Disaster of Bandung Basin Subsurface: Perspective from Geological Approach. *Geol. Ecol. Landsc.* **2025**, *9*, 933–951. [CrossRef]
28. Yurtsever, A.K.; Dabanli, I. Groundwater Level Anomalies as Precursors to the February 6 Double Earthquake in Türkiye. *Environ. Res. Commun.* **2026**, *8*, 025020. [CrossRef]
29. Büyüksaraç, A.; Bektaş, Ö.; Alkan, H. Fault Modeling Around Southern Anatolia Using Aftershock Sequence of Kahramanmaraş Earthquakes (Mw = 7.7 and Mw = 7.6) and Interpretation of Potential Field Data. *Acta Geophys.* **2024**, *72*, 2985–2996. [CrossRef]
30. Şengör, A.M.C. The North Anatolian Transform Fault: Its Age, Offset and Tectonic Significance. *J. Geol. Soc.* **1979**, *136*, 269–282. [CrossRef]
31. Barka, A.A. The North Anatolian Fault Zone. *Ann. Tectonicae* **1992**, *6*, 164–195.
32. Özden, S.; Gündoğdu, E.; Bekler, T. Interactions between Eurasian/African and Arabian Plates: Eskişehir Fault, NW Turkey. *J. Afr. Earth Sci.* **2015**, *111*, 349–362. [CrossRef]
33. Büyüksaraç, A.; Bekler, T.; Demirci, A.; Eyisüren, O. New Insights into the Dynamic Characteristics of Alluvial Media Under the Earthquake Prone Area: A Case Study for the Çanakkale City Settlement (NW of Turkey). *Arab. J. Geosci.* **2021**, *14*, 2086. [CrossRef]
34. Reilinger, R.; McClusky, S.; Vernant, P.; Lawrence, S.; Ergintav, S.; Cakmak, R.; Ozener, H.; Kadirov, F.; Guliev, I.; Stepanyan, R.; et al. GPS Constraints on Continental Deformation in the Africa-Arabia-Eurasia Continental Collision Zone and Implications for the Dynamics of Plate Interactions. *J. Geophys. Res. Solid Earth* **2006**, *111*, B05411. [CrossRef]
35. Emre, Ö.; Duman, T.Y.; Özalp, S.; Şaroğlu, F.; Olgun, Ş.; Elmacı, H.; Çan, T. Active Fault Database of Turkey. *Bull. Earthq. Eng.* **2018**, *16*, 3229–3275. [CrossRef]
36. AFAD Earthquake Catalog. Available online: https://deprem.afad.gov.tr/event-catalog (accessed on 26 May 2026).
37. U.S. Geological Survey. Landsat Data. 2026. Available online: https://earthexplorer.usgs.gov/ (accessed on 20 May 2026).
38. Čejka, F.; Zahradník, J.; Turhan, F.; Sokos, E.; Gallovič, F. Long-Period Directivity Pulses of Strong Ground Motion During the 2023 Mw 7.8 Kahramanmaraş Earthquake. *Commun. Earth Environ.* **2023**, *4*, 413. [CrossRef]
39. Kazaz, İ.; Bilge, İ.H.; Gürbüz, M. Near-Fault Ground Motion Characteristics and Its Effects on a collapsed Reinforced Concrete Structure in Hatay during the February 6, 2023 Mw 7.8 Kahramanmaraş Earthquake. *Eng. Struct.* **2024**, *298*, 117067. [CrossRef]
40. Silahtar, A.; Senkaya, M.; Karaaslan, H. Multi-criteria Decision-Making (MCDM) Model for Building Damages in the Kahramanmaraş 2023 Earthquakes Sequence Based on Soil, Ground Motion and Earthquake Source-Path Parameters. *Bull. Earthq. Eng.* **2025**, *23*, 5137–5159. [CrossRef]
41. Ministry of Environment, Urbanization, and Climate Change. Available online: https://hasartespit.csb.gov.tr/ (accessed on 20 May 2026).
42. IRAP. *Kahramanmaraş İl Afet Risk Azaltma Planı*; AFAD Kahramanmaraş İl Afet ve Acil Durum Müdürlüğü: Kahramanmaraş, Türkiye, 2020.

43. Cetin, K.O.; Ilgac, M.; Can, G.; Cakir, E. (Eds.) *Preliminary Reconnaissance Report on February 6, 2023, Pazarcık Mw = 7.7 and Elbistan Mw = 7.6, Kahramanmaraş-Türkiye Earthquakes*; Report No. METU/EERC 2023-01; Earthquake Engineering Research Center, Middle East Technical University: Ankara, Türkiye, 2023.
44. Baltzopoulos, G.; Baraschino, R.; Chioccarelli, E.; Cito, P.; Vitale, A.; Iervolino, I. Near-source ground motion in the M7.8 Gaziantep (Turkey) earthquake. *Earthq. Eng. Struct. Dyn.* **2023**, *52*, 3903–3912. [CrossRef]
45. Lekkas, E.; Carydis, P.; Vassilakis, E.; Mavroulis, S.; Argyropoulos, I.; Sarantopoulou, A.; Mavrouli, M.; Konsolaki, A.; Gogou, M.; Katsetsiadou, K.; et al. The 6 February 2023 Turkey-Syria Earthquakes. In *Newsletter of Enviromental, Disaster and Crises Management Strategies*; National and Kapodistrian University of Athens: Athens, Greece, 2023; Volume 29, pp. 1–202. Available online: https://www.preventionweb.net/media/86206 (accessed on 20 July 2026).
46. Bilim, F.; Koşaroğlu, S.; Aydemır, A. Relationship Between Crustal Magnetic Anomalies and Earthquake Activity in Malatya and Surrounding Region after the 2023 Kahramanmaraş Earthquakes, Southeastern Türkiye. *Acta Geophys.* **2026**, *74*, 48. [CrossRef]
47. Cetin, K.O.; Soylemez, B.; Guzel, H.; Cakir, E. Soil Liquefaction Sites Following the February 6, 2023, Kahramanmaraş-Türkiye Earthquake Sequence. *Bull. Earthq. Eng.* **2025**, *23*, 921–944. [CrossRef]
48. Erbaş, Y.; Mercimek, Ö.; Anıl, Ö.; Çelik, A.; Akkaya, S.T.; Kocaman, İ.; Gürbüz, M. Design Deficiencies, Failure Modes and Recommendations for Strengthening in Reinforced Concrete Structures Exposed to the February 6, 2023 Kahramanmaraş Earthquakes (Mw 7.7 and Mw 7.6). *Nat. Hazards* **2025**, *121*, 3153–3194. [CrossRef]
49. Senkaya, M.; Okursoy, M.E.; İnkaya, T.; Silahtar, A.; Karaaslan, H. Rule-Based Damage Assessment of the 2023 Kahramanmaraş Earthquakes: A Decision Tree and Association Analysis Approach. *Nat. Hazards* **2026**, *122*, 552. [CrossRef]
50. Arslan, M.H.; Dere, Y.; Ecemiş, A.S.; Doğan, G.; Özturk, M.; Korkmaz, S.Z. Code-Based Damage Assessment of Existing Precast Industrial Buildings Following the February 6th, 2023 Kahramanmaraş Earthquakes (Pazarcık Mw 7.7 and Elbistan Mw7. 6). *J. Build. Eng.* **2024**, *86*, 108811. [CrossRef]
51. Mertol, H.C.; Tunç, G.; Akış, T.; Kantekin, Y.; Aydın, İ.C. Investigation of RC Buildings after 6 February 2023, Kahramanmaraş, Türkiye Earthquakes. *Buildings* **2023**, *13*, 1789. [CrossRef]
52. Bassurucu, M.; Yildiz, O.; Kina, C. Seismic Performance Assessment of an RC Building Due to 2023 Türkiye Earthquakes: A Case Study in Adıyaman, Türkiye. *Buildings* **2025**, *15*, 521. [CrossRef]
53. Eren, M.E.; Fenerli, C. Seismic Failure Mechanism Shift in RC Buildings Revealed by NDT-Supported, Field-Calibrated BIM-Based Models. *Appl. Sci.* **2026**, *16*, 455. [CrossRef]
54. Erdağ, A.; Kardoğan, P.S.Ö.; Ordu, E.; Toklu, K. Post-Earthquake Mechanical Performance and Geological Assessment of Reinforced Concrete Structures Damaged in the 2023 Kahramanmaraş Earthquakes. *Adv. Civ. Eng.* **2026**, *2026*, 4714668. [CrossRef]
55. İnce, E.G.; Çakıl, B.; Şimşek, M.; İnce, O. Evaluation of Ground Motions and Seismic Performance of RC Buildings after 2023 Kahramanmaraş Earthquakes: Design and Construction Deficiencies. *Bull. Earthq. Eng.* **2025**, *24*, 727–754. [CrossRef]
56. Avğın, S.; Köse, M.M.; Çınar, M. Critical Review of Design Practices and Observed Damages in Precast Industrial Buildings: Evidence from the February 2023 Türkiye Earthquakes. *Bull. Earthq. Eng.* **2025**, *24*, 1151–1188. [CrossRef]
57. Akbaş, B.; Akdeniz, N.; Aksay, A.; Altun, İ.E.; Balcı, V.; Bilginer, E.; Bilgiç, T.; Duru, M.; Ercan, T.; Gedik, İ.; et al. 1:1.250.000 ölçekli Türkiye Jeoloji Haritası. Maden Tetkik ve Arama Genel Müdürlüğü Yayını, Ankara, Türkiye. 2011. Available online: https://yerbilimleri.mta.gov.tr/home.aspx (accessed on 25 July 2026).

Disclaimer/Publisher's Note: The statements, opinions and data contained in all publications are solely those of the individual author(s) and contributor(s) and not of MDPI and/or the editor(s). MDPI and/or the editor(s) disclaim responsibility for any injury to people or property resulting from any ideas, methods, instructions or products referred to in the content.